



New empirical stiffness equations for corner-filletted flexure hinges

Q. Meng¹, Y. Li^{1,2}, and J. Xu¹

¹Department of Electromechanical Engineering, Faculty of Science and Technology, University of Macau, Av. Padre Tomas Pereira, Taipa, Macao SAR, China

²School of Mechanical Engineering, Tianjin University of Technology, Tianjin 300384, China

Correspondence to: Y. Li (ymli@umac.mo)

Received: 6 March 2013 – Revised: 13 May 2013 – Accepted: 5 June 2013 – Published: 15 October 2013

Abstract. This paper investigates the existing stiffness equations for corner-filletted flexure hinges. Three empirical stiffness equations for corner-filletted flexure hinges (each fillet radius, r , equals to $0.1l$; l , the length of a corner-filletted flexure hinge) are formulated based on finite element analysis results for the purpose of overcoming these investigated limitations. Three comparisons made with the existing compliance/stiffness equations and finite element analysis (FEA) results indicate that the proposed empirical stiffness equations enlarge the range of rate of thickness (t , the minimum thickness of a corner-filletted flexure hinge) to length (l), t/l ($0.02 \leq t/l \leq 1$) and ensure the accuracy for each empirical stiffness equation under large deformation. The errors are within 6% when compared to FEA results.

1 Introduction

Flexure-based compliant mechanisms (FCMs) are becoming increasingly popular due to their remarkable advantages such as part-count reduction, reduced assembly time, and simplified manufacturing processes in terms of cost reduction, increased precision and reliability, reduced wear and weight, and increased performance (Palmieri et al., 2012; Lobontiu, 2002; Berselli, 2009). In addition, FCMs are the perfect substitutions of traditional rigid mechanisms, compared to the other types of compliant mechanisms. A FCM can not only transform a traditional rigid mechanism in terms of its functions and structure, but also implement high precision and high frequency while the traditional rigid mechanism cannot do. For instance, FCMs are increasingly used in the fields of micro-scale and nano-scale technologies, such as smaller and high precision positioning devices in automobiles, telecommunications, medical, biology, optics or computer industries (Ma et al., 2006; Ivanov and Corves, 2010; Yin and Ananthasuresh, 2003; Lobontiu and Garcia, 2003; Dong et al., 2008, 2005; Xu and King, 1996; Li and Xu, 2009).

A FCM relies on the elastic deformation of its connectors, i.e. the flexure hinges, to perform its functions of transmitting and/or transforming motion and force (Yin and Anan-

thasuresh, 2003). The flexure hinges which are utilized in connecting the rigid components are regarded as the traditional joints in a mechanism, therefore, play a key role in realizing the roles of the mechanism. In spite that flexure hinges own numerous attractive attributes over traditional rigid joints, however, FCMs are not used as widely as rigid-body mechanisms. The main limitation might be the lack of materials and processing techniques that enable structures deform considerably with adequate strength. A lot of researchers put efforts on changing the shape of flexure hinges and studying the stiffness and stress characteristics of these flexure hinges. So far, the flexure hinges can be classified into two categories: the primitive flexure hinges, such as circular flexure hinges, corner filletted flexure hinges, elliptical flexure hinges, parabolic flexure hinges, hyperbolic flexure hinges, “V” shape flexure hinges, right circular elliptical flexure hinges, right circular corner-filletted flexure hinges, two axes flexure hinges, multiple axes flexure hinges, and the complex flexure hinges such as cross axis flexure hinges, cartwheel flexure hinges. The shapes of these flexure hinges can be found in the literatures (Meng et al., 2012; Zettl et al., 2005; Chen et al., 2005; Lobontiu and Paine, 2002; Lobontiu et al., 2002a, 2001, 2002b), this paper will not present them in detail again. Among these flexure hinges, circular flexure

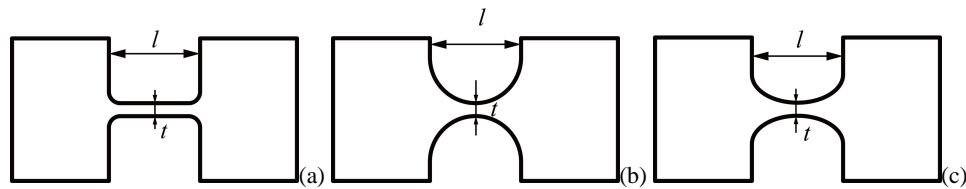


Figure 1. Corner-filletted flexure hinge (a), circular flexure hinge (b) and elliptical flexure hinge (c).

hinges, elliptical flexure hinges and corner-filletted flexure hinges as shown in Fig. 1 are commonly used in FCMs because they are simple and easy to control (Smith et al., 1997; Yong et al., 2008).

This paper addresses the corner-filletted flexure hinges. The stiffness characteristics of corner-filletted flexure hinges with a wide range of t/l are analyzed under different loads applied at the free-end. The influence introduced by shearing is taken into account during the whole analysis. Different ratios t/l are investigated in order to overcome the influence induced by shearing.

The remaining sections of this paper are organized as follows. Section 2 summarizes simply existing research results and some problems need to be resolved in future about corner-filletted flexure hinges. In Sect. 3, fifty finite element analysis models of corner-filletted flexure hinges are built up and their static plane stress analysis is simulated. In Sect. 4, three stiffness empirical equations are formulated by fitting the FEA results. A comparison of the new results together with the previous results is made to FEA in Sect. 5. In the end, the conclusions are drawn in Sect. 7.

2 Literature review

It can be dated back to 1965, Paros and Weisbord firstly presented the compliance-based approach to symmetric circular and right circular flexure hinges by giving the compliance equations and the approximate engineering formulas for these flexure hinges. The analytical approach of monolithic flexure hinges is the landmark in the research of flexure hinges. Particularly, the angles and linear deflections produced on all three axes are expressed in terms of the corresponding external loading.

Ragulskis et al. (1989) analyzed the filleted flexure hinges by applying the static finite element analysis method in order to calculate their compliances (Lobontiu et al., 2001).

In the early work of Howell and Midha (1994), they presented a computer-aided design method to pseudo-rigid-body model that included short length beam. A short length beam can be considered as a corner-filletted flexure hinges without filleted corners at the junction of flexible part and rigid part.

In 1996, Xu and King utilized the topology method to design a flexure-based amplifier for piezo-actuators. Right circular, corner-filletted, and elliptical flexure hinges were analyzed by static finite element analysis (FEA) method. By

comparing both the FEA models to the traditional right-circular flexure hinges, three useful points were presented in their conclusions. They revealed that the corner-filletted flexure hinges are the most accurate in terms of motions relative to the elliptical flexure hinges, the elliptical flexure hinges have less stress for the same displacement and right circular flexure hinges are the stiffest. It is worth to note that the motion described here does not mean the precision of rotation. Even though the corner-filletted flexure hinges provide more accuracy on motion than the elliptical flexure hinges, they present less precision in terms of rotation. The deviation of the rotation center point of a corner-filletted flexure hinges is bigger than a circular flexure hinge.

Lobontiu et al. (2001) did a lot of works on the analysis of corner-filletted flexure hinges. They presented an analytical approach to corner-filletted flexure hinges in order to implement corner-filletted flexure hinges used in piezoelectric-driven amplification mechanisms. In this paper, closed-form in-plane compliance factor equations were formulated based on Castigliano's second theorem. A comparison was made with right circular flexure hinges which revealed that the corner-filletted flexure hinges are more bending-compliant and induce lower stresses but less precise in rotation. Lobontiu and Paine (2002) as well as Lobontiu et al. (2002a, b) also developed the other type of flexure hinges by means of the similar approach as corner-filletted flexure hinges, for instance, cross-section corner-filletted flexure hinges in three-dimensional compliant mechanisms applications, conic-section (circular, elliptical, parabolic and hyperbolic) flexure hinges. In 2004, Lobontiu et al. proposed the closed-form stiffness equations that can be used to characterize the static model and dynamic behavior of single-axis corner-filletted flexure hinges based on Castigliano's first theorem. The new stiffness equations reflect sensitivity to direct- and cross-bending, axial loading, and torsion. Compared to their previous works, the resulting equations for the stiffness factors are more accurate and completely define the elastic response of corner-filletted flexure hinges. No matter how the previous stiffness equations or the refined stiffness equations were presented by the researchers, these equations can be valid only under some assumptions. Two main assumptions are that the deflection subject to shearing is negligible for beam-like structures and the deformations of a flexure hinge are small. Lobontiu and Garcia (2003) presented an analytical model for displacement and stiffness calculations of

planar compliant mechanisms with single-axis flexure hinges relying on the strain energy and Castigliano's displacement theorem. Specifically, circular flexure hinges and corner-fillet flexure hinges as typical symmetric single-axis flexure hinges are contained in the amplifiers in order to verify the deduced stiffness equations.

Du et al. (2011) proposed that a new class of flexure hinges named elliptical-arc-fillet flexure hinges, which covers elliptical arc, circular-arc-fillet, elliptical-fillet, elliptical, circular, circular-fillet (in the other words, corner-fillet, the major axis equals to the minor axis of the elliptical arc), and right circular flexure hinges together under one set of equations. The closed-form equations for compliance and precision matrices of elliptical-arc-fillet flexure hinges were derived in their works. In consequence, the analytical results were within 10% error compared to the FEA results and within 8% error compared to the experimental results. It is worth to note that the closed-form equations were derived based on the small-deformation theory. Therefore, these equations can be valid only when the deformations of the flexure hinges are small enough, or the thickness t to length l ratios are small enough (Du et al., 2011).

With the development of FCMs, the refined design equations under small deflections for typical flexure hinges cannot meet the needs of designers. Large deformation started to be a key problem to develop the typical flexure hinges. Nevertheless, the stiffness characteristics of flexure hinges under large deformation are complex due to shearing deformation. Scholars seek to stay away from the problem in the research. For instance, Trease et al. (2005) proposed a new compliant translational joint in order to overcome the drawbacks of typical flexure hinges such as limited range of motion, axis drift and off-axis stiffness. Compared with the typical flexure hinges, however, the new designed joint is complex. Howell (2002) studied short slender beams under large deformation due to a force or a moment on its free-end. The length of the short beam should be much shorter than the length of the rigid part, while the flexible part should be more compliant than the rigid part. It signifies that the thickness of the short beam should be much less than its length ($t/l \leq 0.1$) (as shown in Fig. 1a).

Tian et al. presented a dimensionless design graph for circular, corner-fillet and cross flexure hinges, based on finite element analysis. The maximum stiffness properties from different hinges in identical situations were described by the FEA results. It revealed that a corner-fillet flexure hinge is preferred over a circular flexure hinge for stiffness demands in a single direction, while the medium stiffness is a cross flexure hinge (Qin et al., 2013; Tian et al., 2010b).

In real applications, however, the existed research results cannot meet some requirements such as stiffness and structure magnitude (the different ratio t/l) determination. Meng et al. (2012) studied the corner-fillet flexure hinges by synthesizing each kind of situation, i.e. the different ratio t/l

and large deformation, under only a pure moment on the free-end.

From the previous works, it can be noted that there are no more accurate design formulas at the stage to estimate stiffness/compliances in the x and y directions for $t/l \geq 0.1$ and the rotational stiffness equation for a vertical force applied at the free end. Therefore, general empirical stiffness equations (named K_θ , K_x and K_y) are formulated in the Sect. 4 based on FEA results to evaluate the stiffness in x and y directions for a wide range of t/l ratios. Also, the rotational empirical stiffness equation will be presented in this section.

3 FEA modeling of corner-fillet flexure hinge

According to the descriptions aforementioned, there are three basic research approaches to the flexure hinges. The first one is based on displacement theorem, the second one is the pseudo rigid body model (PRBM), and the last one is the finite element analysis method. FEA method is used as a benchmark for calculating the rotational stiffness and the stiffness in the x and y directions for flexures. Also, FEA is an important approach to verify these formulas proposed based on the first two research methods. The accuracy of these FEA models was verified by Lobontiu and was with the maximum 8% error compared to three experimental results (Lobontiu et al., 2004). Therefore, this paper studies the stiffness characteristics for corner-fillet flexure hinge with a wide range of t/l under large deformation by means of FEA.

COMSOL software was used to do with FEA of flexure hinges. Fifty corner-fillet flexure hinge models were generated by using two-dimensional, plane stress, parametric analysis, which were moved in the x and y directions. The ratio of t/l for these fifty models are 0.02, 0.04, 0.06, ..., 1, respectively. Please note that the fillet radius, r , for each corner-fillet flexure model is specified to 0.1l in this paper because the fillet radius, r , is used in eliminating the stress concentration at each corner of a hinge. In the work of Meng et al. (2012), the rate of r/l was investigated and the results indicated that the minimum stress happened when the rate of r/l equals to 0.1 under identical material, t/l rate, and deformation conditions. The geometry of one of these analysis models is shown in Fig. 2. The modeled corner-fillet flexure hinges had a depth of 5 mm with a Young's modulus (E) of 1.135 GPa and a Poisson ratio (ν) of 0.33. Triangle element type is more suitable to model irregular shapes and is chosen in this paper to generate the model mesh. Four times refined meshing technique was used to produce automatically refined meshing at parts that high stress concentrations were most likely to occur in order to increase the analytical accuracy (see Fig. 3). The analysis of flexure hinges always is assumed to be cantilever beam. One end is fixed and the other one is free-end. It is easy to figure out that the length of a fixed rigid part cannot be too long because the accuracy of the FEA results can be significantly influenced by the

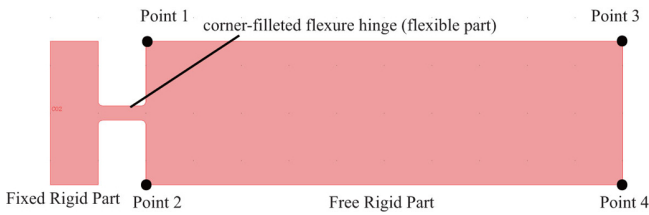


Figure 2. An analytical corner-filleted flexure hinge model.

deformation of this part. On the other hand, the free rigid part should keep it rigid in order to ensure the accuracy of the results. Therefore, the FEA models were designed with a short rigid part at the fixed end and a long rigid part of the fore-end as shown in Fig. 2. The research of corner-filleted flexure hinges under a pure moment applied at the free-end was presented in the previous work. This paper studies corner-filleted flexure hinges under a force in the x or y direction. It is well known that the accuracy of the FEA results can also be influenced by the way the point conditions are assigned to the model. For instance, when a point force in the y direction is applied at the end point of the whole model, an extra moment can be produced in terms of the rotational center point. As for the position where force is applied in the y direction, in this paper, a couple of forces are loaded at the point 1 and point 2, respectively, as shown in Fig. 2. While as for the position where force loaded in the x direction, a couple of forces are applied at the point 3 and point 4. Such loading method can decrease the FEA results error.

4 Empirical stiffness/compliance equations

From the previous section, FEA models with different t/l ratios, which were set from 0.02 to 1 with an increment of 0.02, were generated in COMSOL software. Forces in terms of F_x and F_y were applied at each model and the corresponding deformations, δx and δy were read. Figure 4a, b and c, which shows the relationship between the applied force, the deformation/deflection, and the rate of t/l , indicates that the stiffness is increasing with the increasing deformation/deflection and the increasing geometric parameter t/l . According to the compliance/stiffness equations calculated based on the Castiliagno's displacement theorem (Lobontiu, 2002), the Young's modulus, E , and the width of hinge, w , are proportional to the stiffness around z axis and in x , y directions. Therefore, the product of the two parameters can be divided. Such this, the stiffness can be transformed into a dimensionless quantity. The dimensionless design approach is very popular in the design of FCMs. In addition, the ratio of height to length, t/l , is an important parameter to the stiffness.

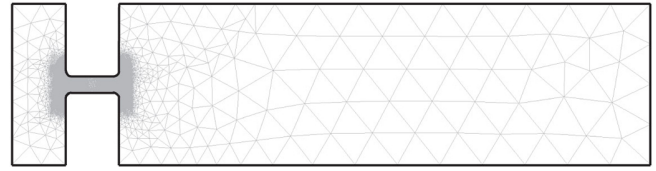


Figure 3. FEA meshing.

4.1 Empirical rotational stiffness equation

The rotational stiffness for corner-filleted here is under the condition of a perpendicular force applied at the end. According to the data in terms of δx and δy read from FEA results, the rotational angles were calculated by means of deforming geometric relationship. The data shown in Fig. 4a is rearranged for stiffness characteristic and the relationship is about rotational stiffness dimensionless design parameter (K_θ/Ew) and the rate t/l as shown in Fig. 5.

It is easy to figure out that the dimensionless design parameter is nearly a function of the rate t/l . While the deviation lies at the end of the relationship curve indicates that the stiffness is related to the deformation. The fourth polynomial, the fifth polynomial, and the sixth polynomial functions were fitted with fitting target of the norm of the residuals, 0.61475, 0.61323, 0.61321, respectively, by means of the data points to formulate empirical rotational stiffness equations. The fitting errors of these fitting functions are shown in Fig. 6. It can be observed from the figure that the minimum fitting error is produced by the sixth polynomial fitting function. The maximum fitting error produced by this fitting function is 2.3474%. In consequence, the sixth polynomial fitting function is chosen as the rotational stiffness design equation as shown in Eq. (1) and its coefficients are shown in Table 1.

$$\frac{K_\theta}{Ew} = \sum_{i=0}^6 a_i \left(\frac{t}{l}\right)^i \quad (1)$$

It is worth to mention that the maximum rotational angle of these FEA models during their deforming is 23° . It means that the influence about shearing deformation was taken into account in the empirical stiffness equation.

4.2 Empirical stiffness equation in x direction

By following the similar procedure as the rotational stiffness, the relationship between the dimensionless design parameter for stiffness in x direction, $K-x/Ew$, and the rate t/l is shown in Fig. 7.

According to the data δx read from FEA results, third, fourth, fifth, sixth, and seventh degrees of polynomial functions were fitted to the fitting target of the norm of the residuals, 0.04339, 0.015942, 0.010882, 0.010003, 0.0098163, respectively. Figure 8 shows the fitting errors for each fitting function. We can figure out from this figure that the minimum fitting errors were produced by the seventh degree

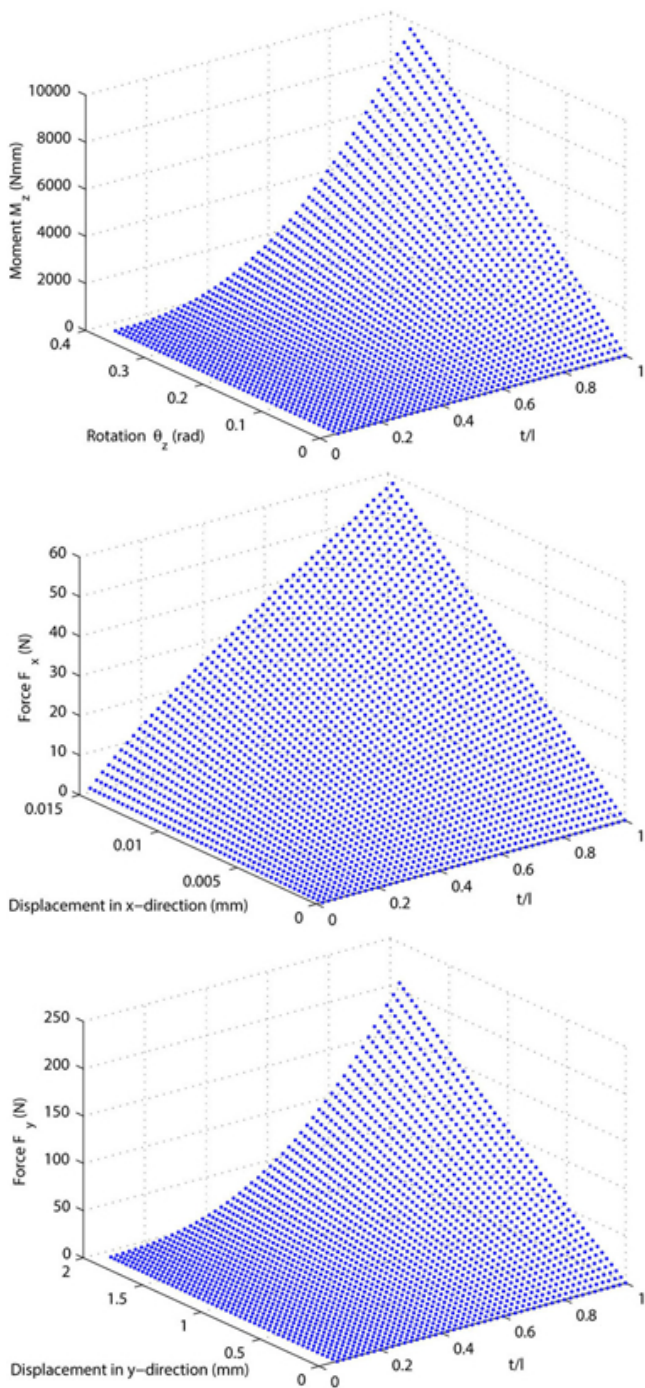


Figure 4. (a) The relationship between M_z , t/l , and rotation angle, θ_z ; (b) The relationship between F_x , t/l , and displacement in x direction; (c) The relationship between F_y , t/l , and displacement in y direction.

polynomial function and the maximum fitting error produced by this function is 0.7213 %. Consequently, the seventh degree polynomial function is chosen as the dimensionless stiffness design equation as shown in Eq. (2) and its coefficients are listed in Table 1.

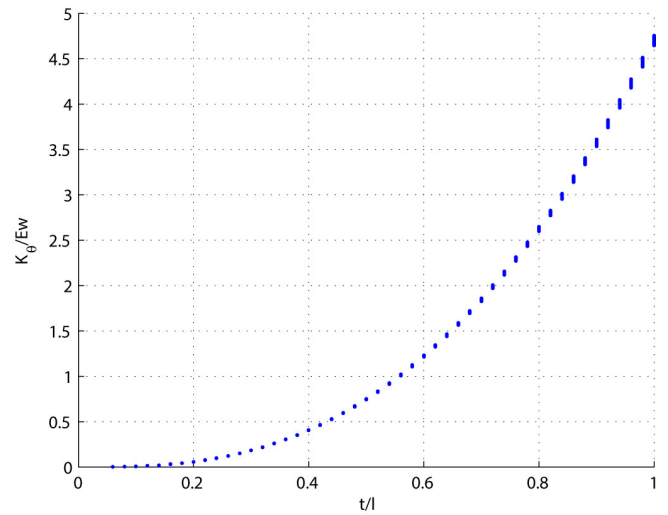


Figure 5. Rotational stiffness dimensionless design parameter.

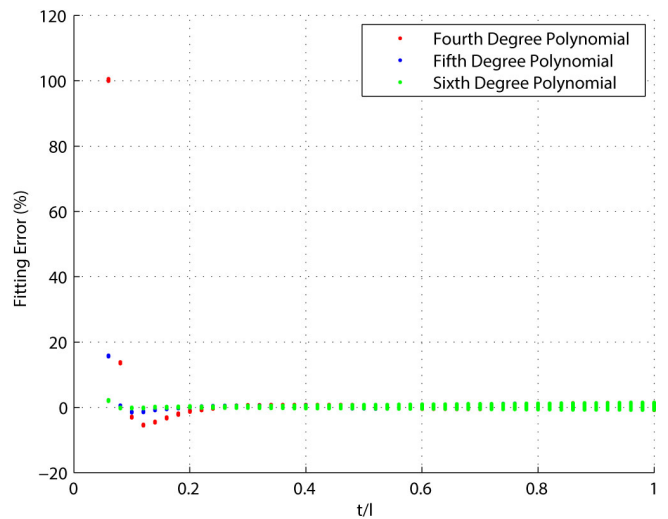


Figure 6. Fitting errors.

$$\frac{K_x}{Ew} = \sum_{i=0}^7 b_i \left(\frac{t}{l}\right)^i \tag{2}$$

4.3 Empirical stiffness equation in y direction

Figure 4c is rearranged for stiffness equation in y direction as shown in Fig. 9. It can be found from this figure that the dimensionless design stiffness parameter K_y/Ew also can be considered as a function of the rate t/l .

However, the deviation which lies on the end part of the curve is larger than the rotational stiffness parameter. It indicates that the stiffness in y direction is related to the deformation of the hinge. In this paper, a simple fitting function

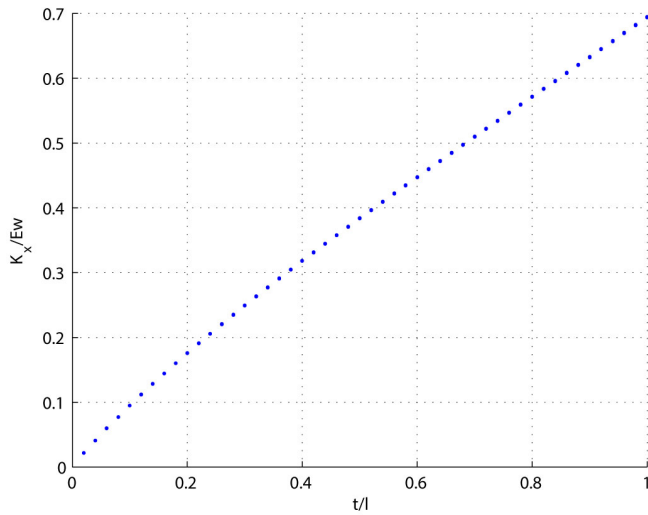


Figure 7. Stiffness in x direction dimensionless design parameter.

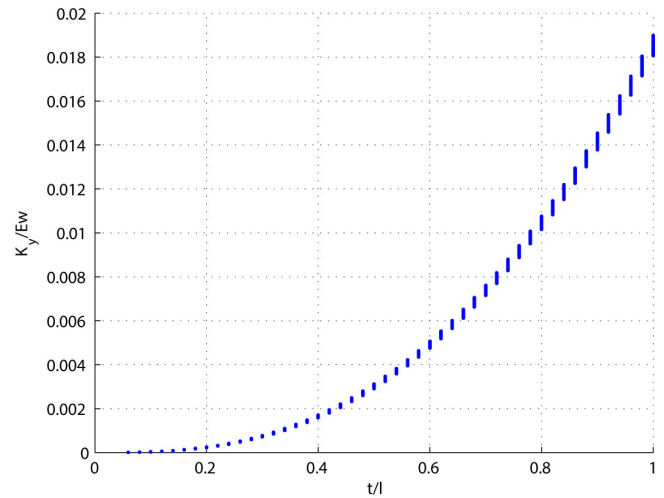


Figure 9. Stiffness in y direction dimensionless design parameter.

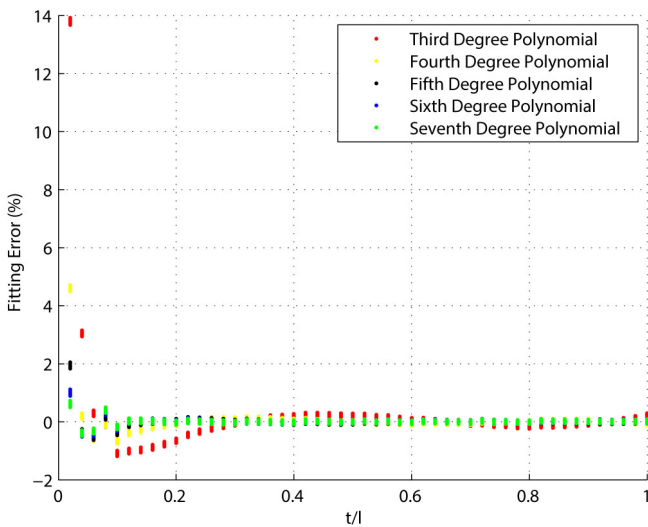


Figure 8. Fitting errors.

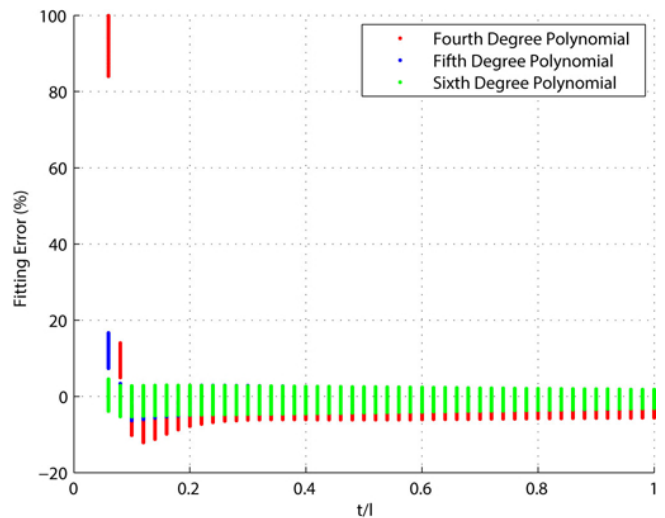


Figure 10. Fitting errors.

was chosen at first. The fourth, fifth, sixth degree polynomial function was fitted with the fitting target of the norm of the residuals, 0.0064273, 0.0064261, and 0.0064261, respectively. The fitting errors are shown in Fig. 10 that shows the minimum errors were produced by the sixth degree polynomial function and the maximum error is 5.2914 %. Therefore, as for the simple fitting function, the sixth degree polynomial function is chosen as the dimensionless stiffness in y direction design equation as shown in Eq. (3) and its coefficients are listed in Table 1.

$$\frac{K_y}{E_w} = \sum_{i=0}^6 c_i \left(\frac{t}{l}\right)^i \quad (3)$$

In order to obtain more accurate fitting stiffness equations, the displacement δ_y is taken into account. By following the

procedure mentioned above, the fitting equation is shown in Eq. (4) and its coefficients are listed in Table 1. Figure 11 shows the fitting error together with the fitting error produced by the simple fitting equation. It shows that the maximum error produced by the complex one is 1.8233 % when the rate t/l is larger than 0.08, while the error is much larger than the one produced by simple fitting equation when the rate t/l is smaller than 0.08. Therefore, the designer can choose the design equation according to the design rate t/l .

$$\frac{K_{cy}}{E_w} = \sum_{i,j=0}^5 \mu_{ij} \left(\frac{t}{l}\right)^i (\Delta y)^j, \quad j \leq 2 \quad (4)$$

It should be noticed that the influence about shearing deformation is taken into account in the empirical stiffness equation.

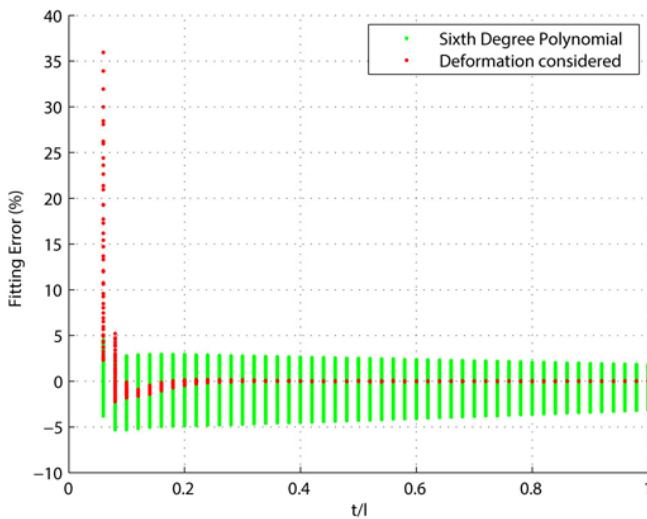


Figure 11. Fitting errors.

5 Comparison of compliance/stiffness results with the previous work and FEA

From Sect. 2, there are a lot of researches in the study of compliance/stiffness characteristics for corner-fillet flexure hinges. This paper adopts the stiffness/compliance equations proposed by Howell (2002), Lobontiu (2002), Du et al. (2011) and Meng et al. (2012) in order to compare to the new empirical stiffness equation. Howell and Midha (1994) proposed stiffness equations for slender beam (it can be considered as a corner-fillet flexure hinge without fillet corners) by means of the pseudo rigid body model. The thickness-length ratio (t/l) is limited to less than 0.1. However, the deflection is not limited. Lobontiu proposed compliance equations by integrating the linear differential equation of a beam. The thickness-length ratio has not been limited. But the deformation must be small. Du et al. (2011) derived the compliance equations based on matrix methods. These closed-form compliance equations for the special configuration which is circular-fillet flexure hinges can be utilized when the thickness(t)-length(l) ratio is less than 0.1. Stiffness equations proposed by Meng et al. (2012) are fitted by means of FEA results based on Lobontiu's equations. Full stiffness equation and simple stiffness equation can be valid even though the deformation is large. However, it is noticed that the loading approach for equations of Howell (2002) and Meng et al. (2012) is a pure moment applied at the end. Therefore, these equations cannot describe the rotational stiffness accurately when a vertical force is applied at the free-end. These stiffness equations are shown in Appendix A, B, C and D.

Table 1. Coefficients for Eqs. (1), (2), (3), and (4).

	Eq. (1)		Eq. (2)		Eq. (3)
a_0	6.10E-04	b_0	1.64E-03	c_0	-1.60E-03
a_1	-1.87E-02	b_1	1.02E+00	c_1	7.78E-03
a_2	2.25E-01	b_2	-1.11E+00	c_2	-1.85E-02
a_3	7.42E+00	b_3	2.28E+00	c_3	3.00E-02
a_4	-4.57E+00	b_4	-3.61E+00	c_4	8.28E-04
a_5	2.11E+00	b_5	3.75E+00	c_5	-6.27E-05
a_6	-4.59E-01	b_6	-2.17E+00	c_6	1.92E-06
		b_7	5.27E-01		
Eq. (4)					
μ_{00}	1.10E-05	μ_{12}	-1.13E-02	μ_{31}	8.71E-03
μ_{01}	-1.28E-04	μ_{20}	1.94E-03	μ_{32}	-1.39E-02
μ_{02}	7.63E-04	μ_{21}	-6.77E-03	μ_{40}	-1.18E-02
μ_{10}	-2.35E-04	μ_{22}	5.02E-02	μ_{41}	-3.80E-03
μ_{11}	1.75E-03	μ_{30}	2.55E-02	μ_{50}	2.67E-03

5.1 Comparison of rotational stiffness equations, M_z/θ_z

Stiffness, M_z/θ_z (or its inverse, compliance, θ_z/M_z) of the corner-fillet flexure hinge as mentioned before was calculated using design equations of Lobontiu (2002), Howell and Midha (1994), Du et al. (2011), full and simple equation of Meng et al. (2012) and the new empirical equation. Their results were compared with the FEA results by the simulation method used in this paper. A corner-fillet flexure hinge, which was with thickness-length ratio t/l equaled to 0.5 and the maximum deforming rotational angle equaled to 23° , is chosen as an instance in order to show the errors induced by these equations. The comparison results are shown in Fig. 12. It shows that the results calculated by the equation of Howell (2002) and Lobontiu diverged greatly from the FEA results. The maximum errors induced by the equation of Howell (2002) and Lobontiu were 40.2252% and 45.787%, respectively, happened on the maximum rotation. The error induced by the compliance equation of Du et al. (2011) is less than Howell's and Lobontiu's, and it is 32.57%. However, the errors induced by full and simple stiffness equations deduced by Meng et al. (2012) are small, and the maximum errors are 3.3292% and 3.6826%, respectively. The minimum error is produced by the new empirical rotational stiffness equation and it is only 0.7955% at the identical situation.

Percentage errors of the comparison of various ratios of thickness-length were plotted in Fig. 13. The figure shows that the equations of Howell (2002) and Du et al. (2011) respectively keep accurate when the thickness-length ratio t/l is less than 0.1; the equation of Lobontiu only keeps accurate when the rotational angle is small enough; and the equations proposed by Meng et al. (2012) can keep accurate whatever high ratio of t/l or high rotation. However, the equations of Meng et al. (2012) are more complex than the new empirical rotational stiffness equations and are less accurate than the

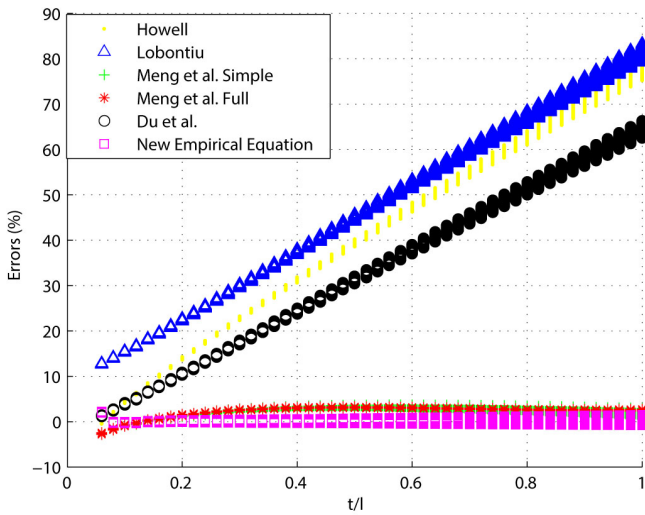


Figure 12. Comparison between FEA results and stiffness equations results $t/l = 0.5$.

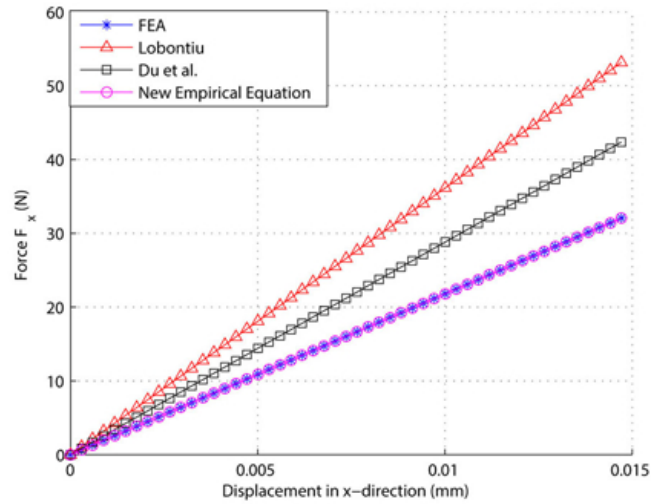


Figure 14. Comparison between FEA results and stiffness equations results $t/l = 0.5$.

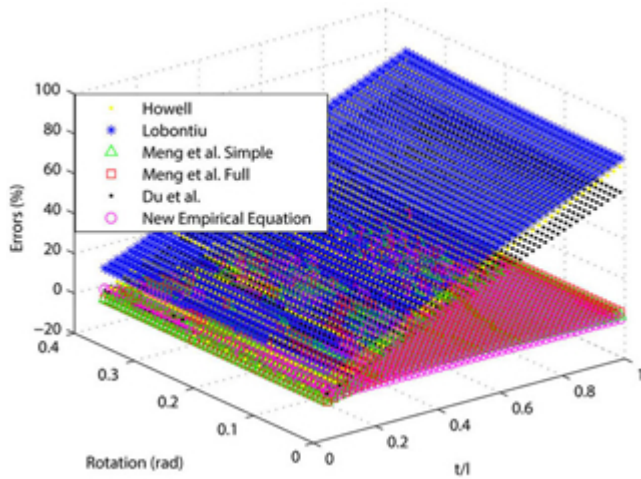


Figure 13. Errors of comparison results.

new one. The maximum errors induced by these equations of Howell (2002), Lobontiu (2002), Du et al. (2011), Meng et al. (2012) full and simple, and new empiric are 79.3530 %, 83.3920 %, 66.3578 %, 3.7248 %, 3.3292 %, and 2.2474 %, respectively.

5.2 Comparison of stiffness equations in x direction, F_x/δ_x

According to the previous comparison approach, the stiffness in x direction, F_x/δ_x of the corner- filleted flexure hinge was calculated using design equations of Lobontiu, Du et al. (2011) and new empirical stiffness equation. Their results were compared with the FEA results by the simulation method used in this paper. As what's described above, the corner- filleted flexure hinge, which was with thickness-

length ratio t/l being 0.5 and the maximum displacement in x direction being 0.0147 mm, was chosen as an instance in order to show the errors induced by these equations. The comparison results are shown in Fig. 14. We can observe that the results calculated by the equations of Lobontiu and Du et al. (2011) diverged greatly from the FEA results. The maximum error induced by the equation of Lobontiu (2002) and Du et al. (2011) were 32.3346 % and 32.1432, respectively, happened on the maximum displacement. However, the new empirical rotational stiffness equation produced only 0.0763 % at the identical situation.

Percentage errors of the comparison for various ratios of thickness-length are plotted in Fig. 15. The figure shows that the equations of Lobontiu and Du et al. (2011) only keeps accurate when the ratio of thickness to length is small enough. However, the results calculated by the new empirical stiffness equation in x direction have not diverged too much from the FEA results. The maximum errors induced by these equations of Lobontiu, Du et al. (2011), and new empiric are 45.2946 %, 45.0941 %, 0.7213 %, respectively.

5.3 Comparison of stiffness equations in y direction, F_y/δ_y

The stiffness in y direction, F_y/δ_y of the corner- filleted flexure hinge was calculated using design equations of Lobontiu (2002), Du et al. (2011) and new empirical stiffness equations (Eqs. 3 and 4) in y direction. Their results were compared with the FEA results by simulation method as described above. It is noticed that the corner- filleted flexure hinge, which was with thickness-length ratio t/l being 0.5 and the maximum displacement in y direction being 1.9226 mm, was chosen as an instance in order to show the errors induced by these equations. The comparison results are shown in

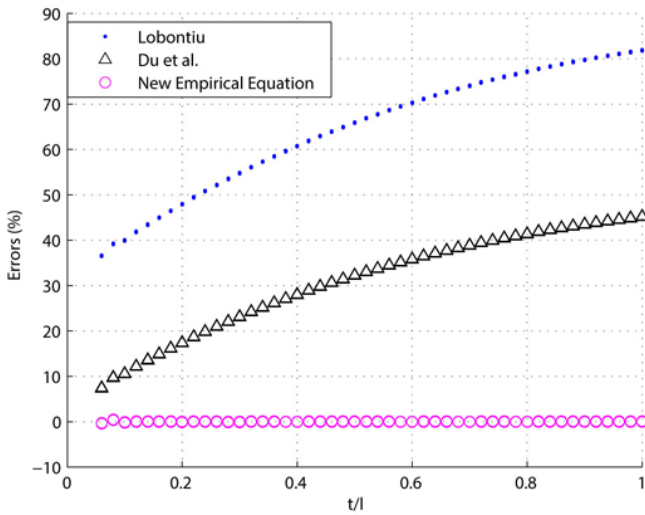


Figure 15. Errors of comparison results.

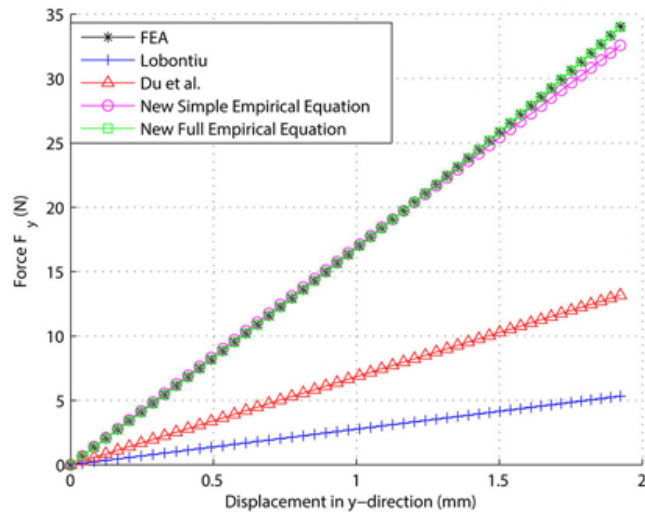


Figure 16. Comparison between FEA results and stiffness equations results $t/l = 0.5$.

Fig. 16. We can see that the results calculated by equation of Lobontiu (2002) and Du et al. (2011) deviate greatly from the FEA results. The maximum error induced by the equation of Lobontiu and Du et al. (2011) were 84.3457 % and 61.2894 %, respectively, happened on the maximum displacement. However, the new empirical rotational stiffness equations produced only 2.49 % and 0.0622 %, respectively, at the identical position.

Percentage errors of the comparison for various ratios of thickness-length were plotted in Fig. 17. The figure shows that the equation of Lobontiu and Du et al. (2011) were not accurate whenever the ratio of thickness to length is small or large. However, the results calculated by the new empirical stiffness equation in y direction have not deviated too much from the FEA results. The maximum errors induced

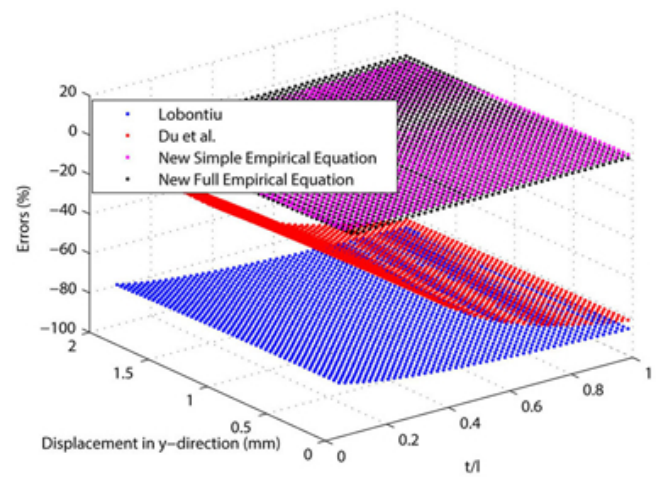


Figure 17. Errors of comparison results.

by these equations of Lobontiu, and new empirical equations are 87.1453 %, 82.8926 %, 5.2914 %, and 1.8233 %, respectively. The errors induced by equations of Lobontiu existed because that the shear compliances/stiffness were not considered in the compliance equations.

To sum up, the suggested stiffness/compliances equations to be used for any particular t/l range and the corresponding minimum, maximum percent errors, were summarized in Table 2.

6 Conclusions

This paper proposes three empirical stiffness equations for a wide range of t/l ratios ($0.02 \leq t/l \leq 1$) and large deformation for corner-filletted flexure hinges with fillet radius $0.1l$ based on FEA results. These three empirical stiffness equations are rotational stiffness equation when a vertical force was applied at the end; stiffness equation in x direction when a force in the x direction was applied at the end; and stiffness equation in y direction when a force in the y direction was applied at the end. These equations were compared to FEA results together with rotational stiffness equations of Howell, stiffness equations proposed by Lobontiu, compliance equations derived by Du et al. (2011) and rotational equations of Meng et al. (2012). Based on the results of comparisons, the proposed empirical stiffness equations are not only more simple than the existed stiffness equations, but also more accurate than others. The percentage errors of these empirical equations were found to be less than 6 % when compared to FEA results. The new proposed empirical stiffness design equations own simple shape and high design precision, which can be easily used in design of flexure-based compliant mechanisms.

Table 2. Suggested stiffness/compliance equations for a particular t/l range.

	t/l	K_θ				K_x			K_y		
		θ_z (rad)	Form	Err _{min} (%)	Err _{max} (%)	Form	Err _{min} (%)	Err _{max} (%)	Form	Err _{min} (%)	Err _{max} (%)
Howell (2002)	(0,0.1]	0.38	Simple	0.13	4.48	N/A	N/A	N/A	N/A	N/A	N/A
Lobontiu (2002a)	(0,0.3]	0.38	Complex	12.57	22.8	Complex	7.28	22.8	Complex	74.21	80.23
Chen et al. (2005)	(0,0.1]	0.38	Complex	1.13	4.13	Complex	7.28	10.64	Complex	9.84	18.87
Meng et al. (2012) (Full)	(0,1]	0.38	Complex	0.12	3.33	N/A	N/A	N/A	N/A	N/A	N/A
Meng et al. (2012) (Simple)	(0,1]	0.38	Complex	0.03	3.72	N/A	N/A	N/A	N/A	N/A	N/A
New Empirical Equation	(0.02,1]	0.38	Simple	3.40E-04	2.25	Simple	5.70E-05	0.5	Simple	2.30E-04	5.29
	(0.08,1]	0.38	N/A	N/A	N/A	N/A	N/A	N/A	Complex	2.50E-05	1.82

Appendix A

Du et al.

Compliance equation in x , y and α_z direction

$$\frac{\Delta x}{F_x} = \frac{a}{Ewb} N_1 + \frac{l}{Ewt}$$

$$\frac{\Delta y}{F_y} = \frac{ka}{Gwb} N_1 + \frac{6L^2 a - 12a(cl + c^2 - a^2)}{Ewb^3} N_2 - \frac{12a^3}{Ewb^3} N_4 + \frac{24a^2 l}{Ewb^3} N_6 + \frac{kl}{Gwt} + \frac{6L^2 l - 2l(l^2 + 6c^2 + 6cl)}{Ewt^3}$$

$$\frac{\Delta \alpha_z}{M_z} = \frac{12a}{Ewb^3} N_2 + \frac{12l}{Ewt^3}$$

where,

$$N_1 = \frac{2(2s+1)}{\sqrt{4s+1}} \arctan\left(\sqrt{4s+1} \tan \frac{\phi_m}{2}\right) - \phi_m$$

$$N_2 = \frac{12s^4(2s+1)}{(4s+1)^{5/2}} \arctan\left(\sqrt{4s+1} \tan \frac{\phi_m}{2}\right) + \frac{2s^3(2s+1)(6s^2+4s+1) \sin \phi_m}{(4s+1)^2(1+2s-2s \cos \phi_m)^2} - \frac{2s^4(12s^2+4s+1) \sin \phi_m \cos \phi_m}{(4s+1)^2(1+2s-2s \cos \phi_m)^2}$$

$$N_4 = \frac{48s^5 + 8s^4 + 20s^3 + 30s^2 + 10s + 1}{2(4s+1)^{5/2}} \times \arctan\left(\sqrt{4s+1} \tan \frac{\phi_m}{2}\right) - \left[\frac{s(2s+1)^2(12s^3 - 12s^2 - 3s) \cos \phi_m}{2(4s+1)^2(2s+1-2s \cos \phi_m)^2} + \frac{-12s^3 + 2s^2 + 6s + 1}{2(4s+1)^2(2s+1-2s \cos \phi_m)^2} \right] \times \sin \phi_m - \frac{\phi_m}{4}$$

$$N_6 = \frac{s^3(\cos \phi_m - 1)[(2s+1) \cos \phi_m - 2s - 1]}{2(2s+1-2s \cos \phi_m)^2}$$

Appendix B

Howell et al.

– Rotational stiffness equation

$$K_H = \frac{Ewt^3}{12l}$$

Appendix C

Lobontiu

– Compliance equation in x direction

$$C_{x,L} = \frac{1}{Ew} \left[\frac{l-2r}{t} + \frac{2(2r+t)}{\sqrt{t(4r+t)}} \arctan \sqrt{1 + \frac{4r}{t} - \frac{\pi}{2}} \right]$$

– Rotational compliance equation

$$C_{\theta_z,L} = \frac{12}{Ewt^3} \left\{ l - 2r + \frac{2r}{(2r+t)(4r+t)^3} \left[t(4r+t)(6r^2+4rt+t^2) + 6r(2r+t)^2 \sqrt{t(4r+t)} \arctan \sqrt{1 + \frac{4r}{t}} \right] \right\}$$

– Compliance equation in y direction

$$C_{y,L} = \frac{3}{EW} \left\{ \frac{4(l-2r)(l^2-lr+r^2)}{3l^3} + \sqrt{t(4r+t)} \left[-80r^4 + 24r^3t + 8(3+2\pi)r^2t^2 + 4(1+2\pi)rt^3 + \pi t^4 \right] / 4\sqrt{t^5(4r+t)^5} + \frac{(2r+t)^3(6r^2-4rt-t^2)\arctan\sqrt{1+\frac{4r}{t}}}{\sqrt{t^5(4r+t)^5}} + \left[-40r^4 + 8lr^2(2r-t) + 12r^3t + 4(3+2\pi)r^2t^2 + 2(1+2\pi)rt^3 + \frac{\pi t^4}{2} \right] / 2t^2(4r+t)^2 + \frac{4l^2r(6r^2+4rt+t^2)}{t^2(2r+t)(4r+t)^2} - \frac{(2r+t) \left[-24(l-r)^2r^2 - 8r^3t + 14r^2t^2 + 8rt^3 + t^4 \right]}{\sqrt{t^5(4r+t)^5}} \arctan\sqrt{1+\frac{4r}{t}} \right\}$$

Appendix D

Meng et al.

– Full rotational compliance equation

$$\Gamma_{Full} = \sum_{i,j=0}^3 u_{ij} \theta_z^i \left(\frac{h}{L}\right)^j \text{ where } u_{ij} = 0 \text{ if } i + j \geq 4$$

$$K_{M,Full} = \Gamma_{Full} K_{\theta_z,L}$$

Where the coefficients u_{ij} are shown in Table 3.

– Simple rotational compliance equation

$$\Gamma_{Simple} = \sum_{k=0}^3 v_k \left(\frac{h}{L}\right)^k$$

$$K_{M,Simple} = \Gamma_{Simple} K_{\theta_z,L}$$

Where the coefficients v_{ij} are shown in Table 3.

Table A1. Coefficients for Full and Simple Equation.

u_{00}	1.016065	u_{03}	-0.043752	u_{20}	0.009576
u_{01}	-0.680692	u_{10}	0.002410	u_{21}	-0.095298
u_{02}	0.292380	u_{11}	-0.018696	u_{30}	-0.003720
u_{12}	0.018095				
v_0	1.018856	v_1	-0.713719	v_2	0.350531
v_3	-0.081827				

Acknowledgements. This work was supported in part by National Natural Science Foundation of China (Grant No. 61128008), Macao Science and Technology Development Fund (Grant No. 016/2008/A1), Research Committee of University of Macau (Grant no. MYRG203(Y1-L4)-FST11-LYM, MYRG183(Y1-L3)FST11-LYM).

Edited by: G. Hao

Reviewed by: Y. Tian and one anonymous referee

References

Berselli, G.: On designing compliant actuators based on dielectric elastomers, University of Bologna, Ph.D. thesis, 2009.

Chen, G. M., Jia, J. Y., and Li, Z. W.: Right-circular corner-filletted flexure hinges, in: Proceedings of the IEEE International Conference on Automation Science and Engineering, 249–253, 2005.

Dong, W., Du, Z., and Sun, L.: Stiffness influence atlases of a novel flexure hinge-based parallel mechanism with large workspace, in: IEEE/RSJ International Conference on Intelligent Robots and Systems, 856–861, 2005.

Dong, W., Sun, L., and Du, Z.: Stiffness research on a high-precision, large-workspace parallel mechanism with compliant joints, *Precis. Eng.*, 32, 222–231, 2008.

Du, Y., Chen, G., and Liu, X.: Elliptical-arc-fillet flexure hinges: toward a generalized model for commonly used flexure hinges, *J. Mech. Design*, 133, 1–9, 2011.

Howell, L. L.: *Compliant Mechanisms*, A Wiley-Interscience Publication, John Wiley & SONS., INC., 2002.

Howell, L. L. and Midha, A.: A method for the design of compliant mechanisms with small-length flexural pivots, *J. Mech. Design*, 116, 280–290, 1994.

Ivanov, I. and Corves, B.: Flexure hinge-based parallel manipulators enabling high-precision micro manipulations, *Mechanisms and Machine Science*, 49–60, 2012.

Li, Y. and Xu, Q.: Design and analysis of a totally decoupled flexure-based XY parallel micromanipulator, *IEEE T. Robot.*, 25, 645–657, 2009.

Lobontiu, N.: *Compliant Mechanisms: Design of Flexure Hinges*, CRC Press, 2002.

Lobontiu, N. and Garcia, E.: Analytical model of displacement amplification and stiffness optimization for a class of flexure-based compliant mechanisms, *Comput. Struct.*, 81, 2797–2810, 2003.

Lobontiu, N. and Paine, J. S. N.: Design of circular cross-section corner-filletted flexure hinges for three-dimensional compliant mechanisms, *J. Mech. Design*, 124, 479–484, 2002.

Lobontiu, N., Paine, J. S. N., Garcia, E., and Goldfarb, M.: Corner-filletted flexure hinges, *J. Mech. Design*, 123, 346–352, 2001.

Lobontiu, N., Paine, J. S. N., Garcia, E., and Goldfarb, M.: Design of symmetric conic-section flexure hinges based on closed-form compliance equations, *Mech. Mach. Theory*, 37, 477–498, 2002a.

Lobontiu, N., Paine, J. S. N., O’ Malley, E., and Samuelson, M.: Parabolic and hyperbolic flexure hinges: flexibility, motion precision and stress characterization based on compliance closed-form equations, *Journal of the International Societies for Precision Engineering and Nanotechnology*, 26, 183–192, 2002b.

- Lobontiu, N., Garcia, E., Hardau, M., and Bal, N.: Stiffness characterization of corner-filletted flexure hinges, *Rev. Sci. Instrum.*, 75, 4896–4905, 2004.
- Ma, H. W., Yao, S. M., Wang, L. Q., and Zhong, Z.: Analysis of the displacement amplification ratio of bridge-type flexure hinge, *Sensor. Actuat. A-Phys.*, 132, 730–736, 2006.
- Meng, Q., Berselli, G., Vertechy, R., and Castelli, P. V.: An improved method for design flexure-baessed nonlinear springs, in: *ASME International Design Engineering Technical Conferences & Computers and Information in Engineering Conference, DETC2012-70367*, 2012.
- Palmieri, G., Palpacelli, M., and Callegari, M.: Study of a fully compliant u-joint designed for minirobotics applications, *J. Mech. Design*, 134, 1–9, 2012.
- Paros, J. M. and Weisbord, L.: How to design flexure hinges, *Mach. Des.*, Nov., 25, 151–156, 1965.
- Qin, Y., Shirinzadeh, B., Zhang, D., and Tian, Y.: Compliance modeling and analysis of statically indeterminate symmetric flexure structures, *Precis. Eng.*, 37, 415–424, 2013.
- Ouyang, P. R., Zhang, W. J., and Gupta, M. M.: Design of a new compliant mechanical amplifier, in: *ASME International Design Engineering Technical Conferences & Computers and Information in Engineering Conference, DETC2005-84371*, 2005.
- Ragulskis, K. M., Arutunian, M. G., Kochikian, A. V., and Pogosian, M. Z.: A Study of Fillet Type Flexure Hinges and their Optimal Design, *Vibr. Eng.*, 3, 447–452, 1989.
- Smith, T. S., Badami, V. G., Dale, J. S., and Xu, Y.: Elliptical flexure hinges, *Rev. Sci. Instrum.*, 68, 1474–1483, 1997.
- Tian, Y., Shirinzadeh, B., Zhang, D., and Zhong, Y.: Three flexure hinges for compliant mechanism designs based on dimensionless graph analysis, *Precis. Eng.*, 34, 92–100, 2010a.
- Tian, Y., Shirinzadeh, B., and Zhang, D.: Closed-form equations of the filleted V-shaped flexure hinges for compliant mechanism designs, *Precis. Eng.*, 34, 408–418, 2010b.
- Trease, B. P., Moon, Y. M., and Kota, S.: Design of large-displacement compliant joints, *J. Mech. Design*, 127, 788–798, 2005.
- Xu, W. and King, T.: Flexure hinges for piezoactuator displacement amplifiers: flexibility, accuracy, and stress considerations, *Precis. Eng.*, 19, 4–10, 1996.
- Yin, L. Z. and Ananthasuresh, G. K.: Design of distributed compliant mechanisms, *Mech. Based Des. Struc.*, 31, 151–179, 2003.
- Yong, Y. K., Lu, T. F., and Handley, D. C.: Review of circular flexure hinge design equations and derivation of empirical formulations, *Precis. Eng.*, 32, 63–70, 2008.
- Zettl, B., Szyszkowski, W., and Zhang, W. J.: On systematic errors of two-dimensional finite element modeling of right circular planar flexure hinges, *J. Mech. Design*, 127, 782–787, 2005.